

RSC Advances



This is an *Accepted Manuscript*, which has been through the Royal Society of Chemistry peer review process and has been accepted for publication.

Accepted Manuscripts are published online shortly after acceptance, before technical editing, formatting and proof reading. Using this free service, authors can make their results available to the community, in citable form, before we publish the edited article. This *Accepted Manuscript* will be replaced by the edited, formatted and paginated article as soon as this is available.

You can find more information about *Accepted Manuscripts* in the [Information for Authors](#).

Please note that technical editing may introduce minor changes to the text and/or graphics, which may alter content. The journal's standard [Terms & Conditions](#) and the [Ethical guidelines](#) still apply. In no event shall the Royal Society of Chemistry be held responsible for any errors or omissions in this *Accepted Manuscript* or any consequences arising from the use of any information it contains.

ARTICLE

Spectroscopic study and electronic structure of prototypical iron porphyrins and their μ -oxo-dimer derivatives with different functional configurations

Cite this: DOI: 10.1039/x0xx00000x

Wei Xu,^a Katarzyna Dziedzic-Kocurek,^b Meijuan Yu,^a Ziyu Wu^{c,a} and Augusto Marcelli^{*d,c,e}Received 00th January 2012,
Accepted 00th January 2012

DOI: 10.1039/x0xx00000x

www.rsc.org/

Metalloporphyrins are networking molecules with strong internal N-H hydrogen bonds that may be used to substitute a metal ion inside a porphyrin ring, forming a metallo complex. The understanding of electronic structures and charge dynamics of porphyrin based molecular architectures is mandatory to clarify biological functions, catalytic processes, and optoelectrical responses in which these molecules are involved. We present here a systematic analysis of the electronic structures and the charge dynamics of two different iron-porphyrins (i.e. protoporphyrin IX and *meso*-tetraphenylporphyrin) with different functional architectures. We investigated these prototypical porphyrins and their μ -oxo-dimer derivatives by means of Fe K-edge X-ray Absorption Near-Edge Spectroscopy (XANES) combined with theoretical calculations. The electronic structure, namely the partial projected density of states and the polarization components were discussed in terms of orbital hybridizations among metal and local ligands. Data show that hydrogens are electron donors while the central metal irons accept electrons. Moreover, the metal axial ligands exhibit different electron behaviors: donors for Cl in prototypical porphyrins and acceptors for O in μ -oxo-dimer derivatives. Actually, the charge dynamics are affected by local metal ligands, but also strongly depend on the mid-range atomic ordering of the porphyrins network. The charge dynamics, evaluated from the self-consistent local potential, is associated to charge transfer mechanisms involving interactions with the axial ligands as well as with the substituents. The quantum chemical topology analysis of the electron localization function (ELF) has been used to identify the distribution of the electron pairs. They are localized around Cl atoms regardless of porphyrin configurations. Charge dynamics and electron localization are fundamental information to deep understanding of the role of porphyrin and porphyrin-like molecules in a wide range of molecular biophysical mechanisms and in materials science processes.

Introduction

Porphyrins are interesting and ubiquitous systems with a variety of chemical and biomedical applications: catalysis (especially Mn, Fe and Pd metalloporphyrins), sensors and biosensors, photodynamic therapy and diagnosis (PDT & PDD) as well as biomimetic models of enzymes, e.g., catalases and cytochromes. Moreover, iron porphyrin complexes are relevant cofactors in many enzymes.¹ Synthetic compounds derived

from octaethylporphyrin [H₂(OEP)], *meso*-tetraphenylporphyrin [H₂(TPP)] or *meso*-tetra(p-totyl) porphyrin [H₂(TTP)] are prototype porphyrins among the most studied in chemistry. For instance, *meso*-tetraphenylporphyrin [H₂(TPP)] has been widely used to model the photo-active side of the hemoglobin molecule² while the protoporphyrin IX (PPIX) and its derivative ferrous-protoporphyrin IX (Fe(II)-TPP) perform oxygen carrying and release functions in

hemoglobin and heme proteins. The sensitivity of protoporphyrin IX against light has been applied as a first generation therapy to treat different forms of cancer and skin diseases, i.e., the photodynamic therapy (PDT). Porphyrin studies have played an important role also in malaria research.³The antimalarial drug chloroquine and its analogues have been shown to interact with the μ -oxo dimer of Fe-PPIX via non-covalent π - π stacking between the quinolinal moieties and the porphyrin rings of the μ -oxo dimer.⁴⁻⁵

The structure and physico-chemical properties of porphyrins are also of tremendous interest in many physical, chemical and biological researches. In order to understand the biological function of these molecules, many studies have been focused on the structural and the dynamical features of porphyrins compounds using X-ray techniques, such as X-ray diffraction, X-ray absorption spectroscopy, inelastic X-ray scattering, nuclear resonant scattering, etc.⁶⁻⁹ All these methods succeeded in refining the structure and obtaining dynamical (structural) factors such as the elasticity of a porphyrin configuration.⁹ Besides the structure, the electronic properties, e.g. the charge transfer in porphyrin systems was also investigated by ultra-fast experiments^{10,11} and theoretical calculations.^{12,13} However, due to the failure of the exchange-correlation potential, it was recognized that the density functional theory is inadequate to evaluate the charge transfers processes.¹² Only through a rigorous refinement of functionals, a qualitative description of the charge transfer can be obtained.¹⁴ However, it remains unclear how and why the hydrogen bonding affects the electronic and geometric configurations of porphyrins.¹⁴ Recently, Wisonet *al.* pointed out that the electronic structure is affected by the sample environment via a solvation effect.¹⁵ Also Mössbauer spectroscopy studies, performed on the complexes we investigated, claimed the occurrence of a solvation effect.¹⁶ As an ideal local structural probe, the X-ray absorption spectroscopy was already used to investigate local structural configurations of porphyrins,¹⁷⁻¹⁹ as well as to identify spin-structures combining Mössbauer data and other magnetic and spectroscopic measurements, etc.¹⁷⁻¹⁹

Metalloporphyrins are networking molecules with strong internal N-H hydrogen bonds that may be used to substitute a metal ion inside a porphyrin ring, forming a metallo complex. To understand the mechanisms underpinning their biological functions, catalytic processes, and opto-electrical responses it is necessary to reconstruct their electronic structures and charge dynamics. Among porphyrin models both [H₂(TPP)] and PPIX systems have been widely studied. However, a comprehensive picture of their electronic structures, key issues to describe the dynamical charge transfer and their outstanding catalytic performances is not yet established. In particular, we considered the ferriprotoporphyrin IX chloride (Fe-PPIX-Cl), the iron-tetraphenylporphyrin chloride (Fe-TPP-Cl) and respective μ -oxo-dimers because of their symmetry (structure) and bonding (Cl⁻ versus O²⁻) contributions. In this presented analysis to clarify the electronic structures of these model porphyrins, we will compare and discuss X-ray Absorption Near-Edge Spectroscopy (XANES) spectra, theoretical Full

Multiple Scattering (FMS) calculations and first principles calculations.

Methods

1. Sample preparation, X-ray absorption experiments and photoreduction effects

In the next we define Fe-PPIX-Cl as porphyrin-1 and the μ -oxo-dimer, i.e., the system where the chlorine atom is replaced by an oxygen atom binding the next metallo-porphyrin unit, as porphyrin-2. The Fe-TPP-Cl and, as in the previous case, Fe-TPP μ -oxo-dimer were named porphyrin-3 and porphyrin-4, respectively (Fig. 1). All samples were purchased from *Alfa Aesar* except porphyrin-2 that was synthesized at the department of Biochemistry of the University of Agriculture in Kraków. For the purpose of Mössbauer experiments, the isotope ⁵⁷Fe was used for synthesis. Iron porphyrin dimers were prepared by insertion of iron atoms from ⁵⁷FeCl₃ into protoporphyrin IX (PPIX) (*Sigma-Aldrich*), precipitated from a water-N,N-dimethylformamide (DMF) solution, according to the modified Adler and Fleisher procedure.¹⁷ The reactant solvent obtained in a basic synthetic procedure was treated with a stoichiometric amount of NaOH and diluted with distilled water and centrifuged. Supernatant and sediment were checked at every stage by UV/Vis absorption spectroscopy to monitor the metallization/dimerisation process and later lyophilized.

To perform X-ray absorption experiments samples (both as basic and as powder lyophilized forms) were spread homogeneously onto a Kapton film and sealed. Data were collected at the beamline A1 at Hasylab-DESY in Hamburg operated by the synchrotron radiation storage ring DORIS III. A double crystal Si(111) monochromator was employed to scan the energy around the Fe K-edge (7112 eV) with the nominal energy resolution of 0.5 eV. The absorption energy was calibrated using a Fe foil and measurements were performed in the fluorescence mode with a 7-element HPGe-detector. We checked possible photoreduction induced phenomena in the XANES spectra without success. To rule out the problems of the photoreduction sometimes addressed in the literature on porphyrins systems during x-ray irradiation¹⁵ we also performed on the same samples X-ray Absorption Spectroscopy experiments at the Fe K edge at the B18, the Core XAS beamline of the Diamond Light Source (UK). This synchrotron radiation source operates in the top-up mode at the electron energy of 3 GeV with ~250 mA current. Samples were prepared as previously and spectra were collected at room temperature using a double crystal monochromator equipped with two Si(111) crystals in unfocused mode illuminating the sample with 1011 ph/s on a spot of about 1x1 mm². In the experimental condition we used, the power density at B18 is comparable to that delivered by the DORIS III source. The acquisition of Fe K-edge spectra has been performed in the continuous scan mode (i.e., Quick EXAFS mode) in transmission at normal incidence. The energy resolution of the experimental setup is about 1 eV at the Fe K-edge (7112 keV). Normalized XANES

spectra show no detectable spectral differences within two hours of continuous X-ray irradiation. As it is shown in Fig S1-S3, within the error and with a time resolution of ~ 120 seconds, we confirmed that no photoreduction effects have been detected in the investigated porphyrin samples.

2. The computational methods

Fe *K*-edge XANES spectra were calculated in the framework of the full multiple scattering (FMS) theory based on the muffin-tin potential approximation. We used the crystal structures of porphyrins as available from the Cambridge Structural Database (CSD) for the calculation of the XANES spectra as well as for First Principles calculations (see next section). The atomic potential was calculated using the self-consistent field (SCF) itinerant method, as implemented in the FEFF9.0 code.²¹ Then the energy-dependent Hedin-Lundqvist potential²² (self-energy) was added to account for the inelastic losses of photoelectrons. To achieve a good convergence, the cluster radii of SCF and FMS were 4 Å and 8 Å, respectively. In order to overcome the difficulties in the estimation of the charge transfer based on the Density Functional Theory¹², we used an alternative method based on a self-consistent calculation of the atomic potentials and the muffin-tin approximation. In this way the charge transfer in the atomic cluster can be achieved by subtracting the SCF density defined by the muffin-tin radii from the overlapped atomic charge density.²³

The first principles calculation was carried out using the CASTEP code²⁴ within the local density approximation (LDA) of exchange-correlation functionals.²⁵⁻²⁶ The ultrasoft pseudopotential²⁷ was employed for all atoms using basic electronic configurations, e.g., $1s^1$ for H, $2s^2 2p^2$ for C, $2s^2 2p^3$ for N, $2s^2 3p^4$ for O, $3s^2 3p^5$ for Cl and $3d^6 4s^2$ for Fe with the plane wave basis cut-off at 300 eV. The electronic states were calculated using a Gaussian smearing scheme with a width of 0.1 eV. The geometric structures of crystals were firstly optimized to achieve the energy convergence at 1×10^{-6} eV per atom. Then the density of states, the electron localization function as well as other electronic properties, were calculated using the optimized structures. Density Functional Theory was extensively applied to resolve the electronic structure of porphyrin-related chemicals.²⁸⁻³⁰

3. The structural porphyrin model

We studied four porphyrins (Fig.1, Figure.S1) each of them containing an iron ion in their centers but different substituents (see Fig. 1. a-d): (a) porphyrin-1: Fe-PPIX-Cl (iron protoporphyrin IX chloride) with 2 vinyl, 4 methyl and 2 propionic acid groups attached at β -positions and an axially bonded Cl to the iron center; (b) porphyrin-2: this porphyrin inherits all structural features of porphyrin-1 but oxygen replaces Cl connecting two planes of porphyrin rings (μ -oxo-dimer of porphyrin-1); c) porphyrin-3: the Fe-TPP-Cl, iron-*meso*-tetraphenylporphyrin chloride, contains outer phenyl rings attached to the porphyrin macrocycle with the Fe-Cl bond out of the plane; and d) porphyrin-4: a μ -oxo-dimer of the porphyrin-3.

All parameters of the unit cell of these crystal structures are listed in Table S1. The crystal structure of porphyrin-1³¹ and porphyrin-2³² share the triclinic symmetry group, whereas porphyrin-3³³ and porphyrin-4³⁴ crystallize in the monoclinic and the orthorhombic phase, respectively.

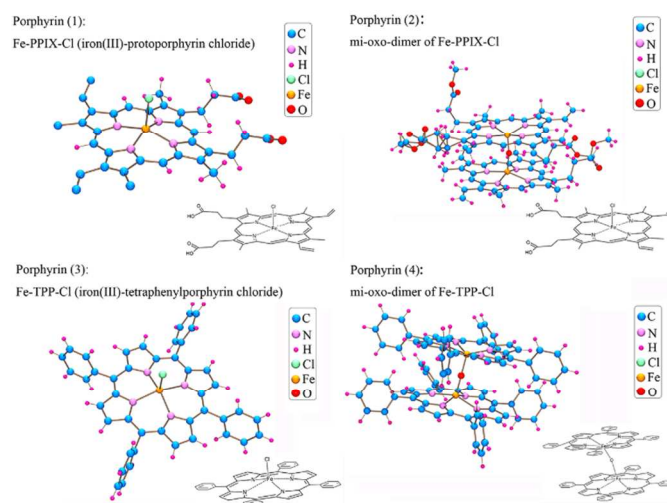


Fig.1 Molecular structures of the four investigated porphyrin complexes.

The relative position of the substituents determines the symmetry of these molecules and the size of the unit cell.

Results and Discussions

1. XANES spectra and FMS simulations

Theoretical spectra have been simulated in the framework of the Full Multiple Scattering (FMS) theory starting from the model structure given in Table S1.

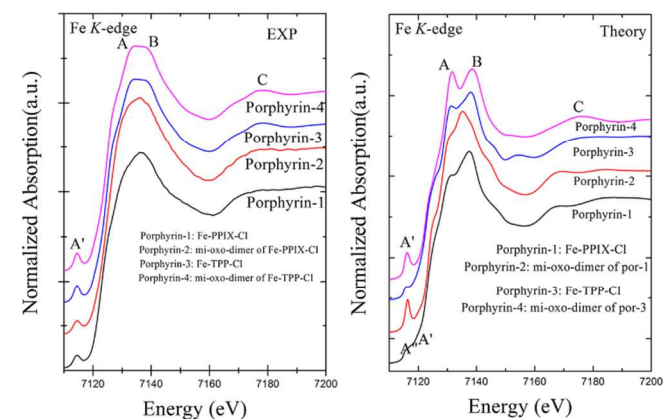


Fig.2 Comparison of experimental (left) and theoretical (right) spectra of the four investigated porphyrin complexes.

Fe *K*-edge XAS spectra probe the transition of $1s$ core electrons to the $4p$ empty states of iron and, as shown in Fig.2, in spite of the difference in the relative intensity of some spectral features, e.g., the pre-edge feature A' , almost all experimental spectra

are in good agreement with FMS simulations. The pre-edge feature A' originates from the transition of 1s core electrons to hybridized Fe 3d states and ligands orbitals of p character.³⁵ Because the hybridization between iron d and chlorine p states is much weaker than between Fe and O the pre-edge feature of oxygen-bridged dimers (porphyrin-2 and porphyrin-4) is more pronounced than that of Fe-PPIX-Cl and Fe-TPP-Cl monomers (porphyrin-1 and porphyrin-3).¹⁵

The shoulder A in the Fe K-edge spectra is more pronounced in TPP (porphyrins 3&4) than in PPIX (porphyrins 1&2) while the following B and C features are not completely resolved in the experimental spectra, due to both spectral resolution and intrinsic disorder, merging in a unique broad structure in the two TPP porphyrin spectra. The features B and C arise from FMS scattering contributions with neighboring atoms located at a relatively large distance from the absorber. Theoretical simulations show that both features could be distinguished also in these compounds and other contributions also appear in the range 7130-7150 eV. Looking at Table S1 and, as shown in Fig. 1, the substituents of the macrocycle in PPIX and TPP porphyrins are β -alkyl groups and phenyl rings, respectively. Simulations indicate that features B and C merge in the PPIX porphyrin in which substituents are β -alkyl groups; on the other hand, a clear split of features B and C occurs in TPP porphyrins, which substituents are peripherally *meso*-substituted phenyl rings. Considering MS contributions from substituents, the split of the features B and C points out the existence of anaperipherally substituted ring structure. On the other hand, due to the broadening the TPP porphyrins (3&4) have a plateau-like shape while PPIX porphyrins (1&2) exhibit a single broad shape at the white line that masks the underlying FMS contributions evident in the other two porphyrins. Data obtained with Mössbauer spectroscopy and SQUID measurements [²⁰& unpublished data of porphyrin-4] point out that, beside the main contribution of μ -oxodimerized molecules, porphyrin-2 and porphyrin-4 contain porphyrins in a monomer form, i.e., without Fe-O-Fe bonds. This result may explain the observed discrepancy between theoretical and experimental spectra in Fig.2.

2. Polarization analysis

The porphyrin structure consists of a macrocycle with its in-plane-substituents and out-of-plane ligands, which in our two systems are chlorides and bridging oxygen atoms. To achieve a better understanding of these local structures we performed x-ray absorption polarized experiments to identify and separate for each spectral features, in and out of plane contributions. In Fig.3, we show polarized Fe K-edge XANES spectra of the four porphyrins. Because of their strong anisotropic structure, in-plane and out-of plane contributions of porphyrin structures can be identified and correlated to the hybridization among iron and different ligands.

Polarized pre-edge features are different among these porphyrins. For both Fe-PPIX-Cl (porphyrin-1) and Fe-TPP-Cl (porphyrin-3), the intensity of the pre-edge feature A in the E//ab component is much stronger than the intensity of the

counterpart in the perpendicular polarization ($E \perp ab$ plane). This difference points out the occurrence of a strong in-plane hybridization between iron and nitrogen atoms. On the other hand, the intensity of the pre-edge feature of μ -oxo-dimer porphyrins in the perpendicular plane component ($E \perp ab$), is comparable to that of the in-plane component (E//ab) for the porphyrin-2 while the first ($E \perp ab$) is stronger than second component (E//ab) in the porphyrin-4. In other words, the hybridization between iron and bridging oxygen atoms is the dominant electronic interaction in μ -oxo-dimer porphyrins.

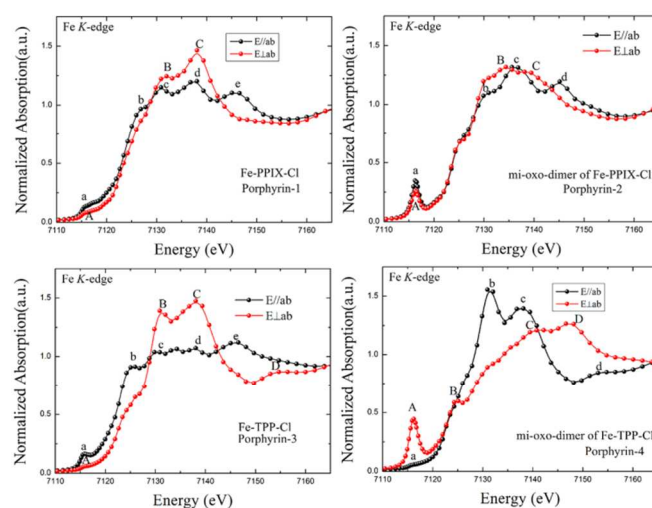


Fig.3 Polarized parallel and perpendicular Fe K-edge XANES spectra of the four porphyrins.

Features in the spectra polarized parallel or perpendicular to the *ab* plane depend also on the local atomic configurations as well as on the substituents. Comparison of porphyrins and their μ -oxo-dimers allows distinguishing the different local structure contributions. In the E//ab spectra, PPIX-Cl and TPP-Cl porphyrins show additional structures respect to the μ -oxo-dimers. In the $E \perp ab$ spectra, characteristic features of PPIX-Cl and TPP-Cl porphyrins, merging in the μ -oxo-dimers, are observed in the range 7130-7140 eV. Furthermore, the substituents' contributions appear from the comparison of $E \perp ab$ spectra of Fe-PPIX-Cl and Fe-TPP-Cl. Indeed, when the substituents are the peripherally *meso*-substituted phenyl rings as in the Fe-TPP-Cl porphyrin, both peaks B and C split, as well as the distinctive feature D associated to scattering contributions from the substituents.

3. Projected Density of States

As discussed above, the orbital hybridization plays an important role in the shape of the pre-edge at the Fe K-edge. To confirm and improve the description, we calculated the density of states projected on each atomic orbital of PPIX and TPP porphyrins (Fig.4 and Fig.5, respectively) and compared them with those of the corresponding μ -oxo-dimers.

By referring to the polarization analysis of Fig. 3, the E//ab components of porphyrin-1 exhibits a stronger pre-edge,

compatible with a larger in-plane hybridization among Fe *d* and N *p* states, in agreement with the projected density of states in Fig. 4. In addition, the pre-edge feature A' of the porphyrin-2 is mainly due to the hybridization of Fe *d* states with bridging O *p* states and, with N and C *p* states.

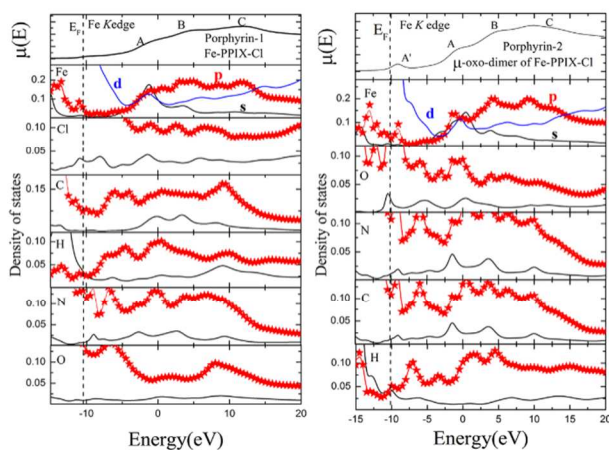


Fig.4 The partial projected density of states of Fe-PPIX-Cl porphyrin (left) and its μ -oxo-dimer derivative (right); the black, red, and blue curves are the s, p and d orbitals contributions, respectively.

In comparison with the Fe-PPIX-Cl porphyrin-1, the hybridization between Fe *d* states and N *p* states is stronger in the Fe-TPP-Cl porphyrin-3 (see Fig. 5, left panel). The pre-edge feature of the μ -oxo-dimer is actually dominated by the hybridization between Fe *d* states and bridging O *p* states. Moreover, the shoulder A in Fig. 4 and 5 can be assigned to Fe p and d states hybridized with O *p*, N *p* and C *p* states. For sake of clarity, the total density of states is showed in the Fig. S4.

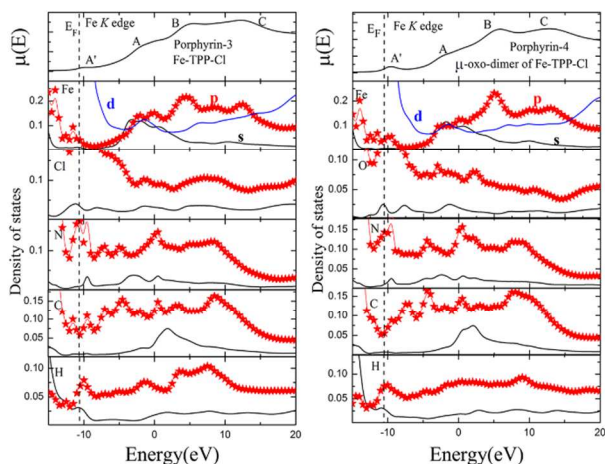


Fig.5 The partial projected density of states of Fe-TPP-Cl porphyrin (left) and its μ -oxo-dimer derivative (right); the black, red, and blue curves are the s, p and d orbitals contributions, respectively.

4. Charge transfer

After the discussion on their structures, in this section, we focus on the charge transfer (CT) that accounts for the charge difference between the ground state charge configuration and

the redistributed charge that guarantees the achievement of a consistent potential.

The sign of the charge transfer indicates if electrons are donated (+) or accepted (-). From our calculation, the charge transfer is the average charge transfer per single atom. The overall charge transfer of each element can be obtained by multiplying the number of specific atoms by their atomic charge transfer. In this way, we may provide a new perspective on the electronic dynamics of a molecular complex. It should be underlined here that from the chemical point of view, terms like accepting or donating electrons can be associated only to functional groups. Here we used donor and acceptor concepts to discuss the atomic charge disproportionation or the charge redistribution associated to different atomic configurations, rather than to “functional acceptor or donor electrons”.

In Fig. 6 we compare the charge transfers of atoms in the four porphyrins, attempting to reconstruct the charge dynamics among the monomer porphyrins and their μ -oxo-dimers. Fe, O, N and C atoms in the four porphyrins investigated are all electron-acceptors regardless of the difference in the iron local environment.

The oxygen atoms bridging two macrocycle rings accept electrons in the μ -oxo-dimers of Fe-PPIX and Fe-TPP porphyrins. By contrast, hydrogen, the most abundant porphyrin element, donates electrons to the system. The Cl atoms bonded with Fe are also donors in both Fe-PPIX-Cl and Fe-TPP-Cl porphyrins.

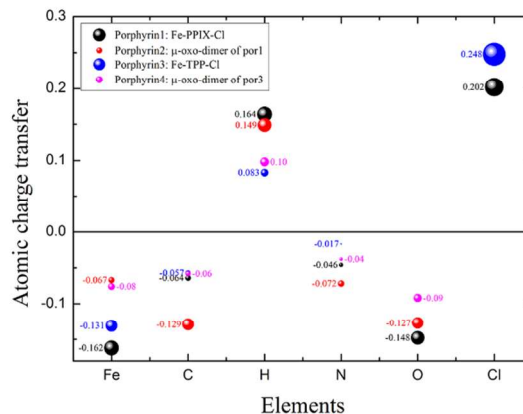


Fig.6 Comparison among porphyrin atomic charge transfers. The dimension of the sphere is proportional to the absolute value of the calculated charge transfer.

In summary, H and Cl are electron donors while all other atoms are acceptors. However, due to the oxygen bridging effects the type and amount of charge transfer is different. For both Fe-PPIX-Cl and Fe-TPP-Cl, H and Cl atoms transfer electrons to Fe, C and N atoms, while electrons donated by H are accepted by Fe, O, N and C in oxygen bridged dimers. Consequently, the CT of Fe and H atoms is larger in porphyrin-based chlorides than in the corresponding μ -oxo-dimers

derivatives, while the CT of C and N are larger in μ -oxo-dimers than in the corresponding chlorides.

Finally, we examined the CT variation due to the substituents morphology. As mentioned above, substituents in TPP porphyrins are peripherally *meso*-substituted phenyl rings while in PPIX porphyrins are β -alkyl groups. For chlorides, the CT of all atoms except Cl, i.e., Fe, C, H, N, is larger in the PPIX than in TPP porphyrin. For their derivative μ -oxo-dimers, the CT of all atoms except Fe, i.e., C, H, N, O is also larger in the PPIX than in the TPP porphyrin. Accordingly, the charge interactions among C, H and N are larger in porphyrins with β -alkyl groups (PPIX porphyrins) than in structures (TPP porphyrins) characterized by phenyl rings as substituents. Moreover, the CT of Fe is larger in Fe-PPIX-Cl than in Fe-TPP-Cl, while the CT of Fe in the μ -oxo-dimer of Fe-PPIX-Cl is slightly lower than that of Fe-TPP-Cl. (Table.S2)

5. Electron localization function

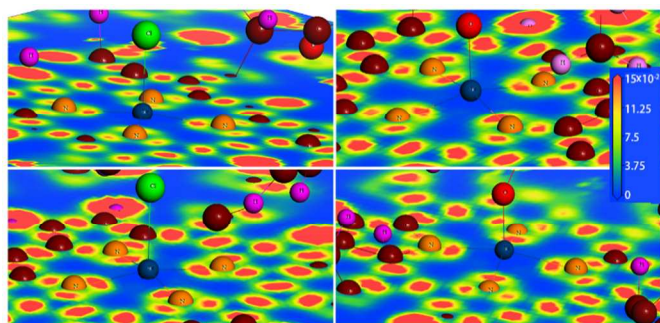


Fig.7 Comparison among electron localization functions projected in the Fe-N ring plane for Fe-PPIX-Cl, Fe-TPP-Cl and their μ -oxo-dimers. The isolevel is set to 0.6.

The electron localization function (ELF) is a mathematical tool capable to identify the localization of the electron pairs in a multi-electron system. The ELF topological analysis has been widely applied to visualize bonds, lone-pairs, etc.

In Fig. 7 and 8 we visualized cross sections of the three dimensional ELF (Fig.S5, Fig.S6) in the two orthogonal directions. The first one is the plane that contains the Fe-macrocycle ring with its substituents while the second is the orthogonal plane containing either Cl atoms in porphyrin-1 and 3, or O atoms in porphyrin-2 and 4.

Looking at the cross sections we may claim that electron pairs in the Fe-macrocycle porphyrin ring are present in all porphyrins. As shown in Fig. 7, three lobes separated by 120° can be clearly identified around N atoms. They represent lone electron pairs of N atoms.³⁶In Fig.8, crescent-shaped lone electron pairs appear around nitrogen towards the bonded iron atoms. Some specific electron pairs are also found around H atoms, as showed in Fig. S5 and S6. Electron pairs around Cl and O atoms are also very peculiar. Indeed, Cl atoms in the Fe-PPIX-Cl and Fe-TPP-Cl structures are decorated with dumb-bell shaped electron pairs while bridging O atoms in the corresponding μ -oxo-dimers are characterized by very weak

electron pairs. This clear difference points out that the Fe-O bond in both oxygen dimers is weaker than the Fe-Cl bond.

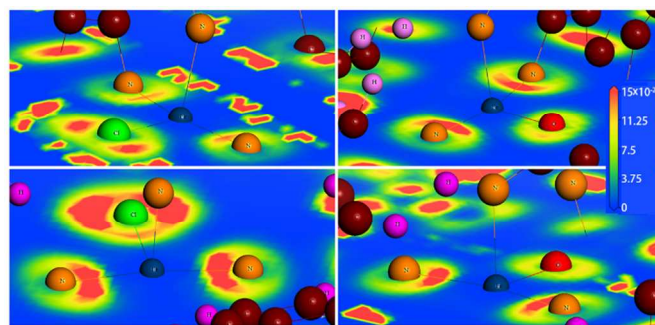


Fig. 8. Comparison among electron localization functions projected in the plane perpendicular to the Fe-N ring and containing Cl or O atoms, for Fe-PPIX-Cl, Fe-TPP-Cl and their μ -oxo-dimers. The isolevel is set to 0.6.

Conclusions

Spectroscopic methods and density functional theory have been used to investigate the electronic structure of two sets of prototype porphyrins characterized by Fe-Cl bonds: Fe-PPIX-Cl, Fe-TPP-Cl and μ -oxo-dimers that contains also β -alkyl groups and *meso*-substituted phenyl rings as substituents. In particular, the dimer structures where Cl atoms are replaced by oxygen atoms are characterized by bridging O atoms bonded to Fe. Starting from their structural similarity and differences, we reconstructed electronic states hybridization, electron pairs localization and charge transfers in the framework of the multiple scattering theory and of the density functional theory.

The analysis of the XANES spectral features at the Fe K-edge allowed describing the atomic interactions in different local configurations (monomer vs. dimer) or substituents contributions (PPIX vs. TPP). Because of the shorter Fe-O bond and due to the strong interaction between Fe and the bridging O, an intense pre-edge appears in the dimer structures compared to their monomer counterparts. Moreover, whereas the local ligand tunes the pre-edge hybridizations, multiple scatterings due to substituents contribute to the shape of the main-peak. Consequently, the TPP porphyrins, characterized by *meso*-substituted phenyl rings, have a double-structure main absorption peak whereas PPIX porphyrins, characterized by "chain-like" β -substituents, have only a broad main absorption feature.

Owing to the strong anisotropic structure of porphyrin structures, the absorption coefficient is anisotropic. In the monomer structures, the in-plane Fe-N hybridization dominates over the hybridization between iron *d* and chlorine *p* states (hereafter called Fe-Cl hybridization). In addition, the out-of-plane Fe-O hybridization is larger in dimers. From the analysis of the polarized XANES spectra we claim that the contribution of substituents is associated to the appearance of a spectral feature at ~ 7150 eV in the out-of-plane spectra. On the contrary, while in the out-of-plane spectrum monomers are characterized by a double-peak, in the corresponding dimer spectrum the main structure in the out-of-plane spectrum

merges or disappears. In agreement with the different configurations of the substituents, a closely inspection of the projected density of states shows that the in-plane hybridization between Fe *d* and N *p* states is stronger in the TPP porphyrin respect to the PPIX porphyrin. Meanwhile, the strong hybridization between Fe and bridging O also gives a contribution.

Furthermore, the charge transfer as well as the localization of electron pairs is associated to ligands and substituents. In monomers, Cl atoms are electron donors regardless of the type of the substituents. On the contrary, all oxygen atoms in dimers are electron acceptors. Interestingly, Fe atoms accept electrons while H atoms are donors both in monomers and dimers. Due to the donor's role of Cl in monomers, the size of the charge transfer towards iron is larger in monomers than in dimers. Moreover, due to the different configuration of substituents, the PPIX porphyrin and its μ -oxo-dimer exhibit a larger charge transfer on Fe, H and N. While almost no localized electron pairs are present around O in dimers, a strong localization of electron pairs around Cl atoms occurs in monomers. Finally, electron pairs are localized around N atoms of Fe-N pyrrole rings in both monomers and dimers, suggesting the occurrence of a strong Fe-N bond.

The experimental results and the theoretical simulations we presented provide an advanced and accurate reconstruction of the electronic structure of monomer and dimer porphyrins, in a framework of different functional groups. We also attempted to describe the interplay among atoms, charge transfer and local configurations of porphyrins, which is fundamental information to understand the mechanism underlying the catalytic and biological functions of these prototypical iron-porphyrins. In addition to previous structural or electronic studies of specific porphyrins, this research describes a unified scenario of the electronic structure and charge transfer mechanisms of two sets of prototypical porphyrins. We demonstrate that symmetry and network structure of a porphyrin molecule are strongly correlated with the electronic properties. Thus, the entire molecular architecture and the details of the functional groups, both peripheral and axial, determine the porphyrin behavior as observed in many chemico-physical processes and phenomena.

Acknowledgements

This work has been financially supported by the National Natural Science Foundation of China (Grant No. 11105172, 11205186), HASYLAB-DESY under the contract RII3-CT-2004-506008, EC (FP7/2007-2013) under grant agreement No. 312284 (DESY, Hamburg) and the grant No. 7150/E-338/M/2013 of the Polish Ministry of Science and Higher Education. We sincerely acknowledge G. Cibin for the support during experiments performed at Diamond within the proposal sp9050.

Notes and references

^aBeijing Synchrotron Radiation Facility, Institute of High Energy Physics, Beijing, 100049, China.

^bM.Smoluchowski Institute of Physics, Jagiellonian University, Reymonta 4, 30-059 Kraków, Poland.

^cNSRL, University of Science and Technology of China, Hefei 230026, China

^dLaboratori Nazionali di Frascati - INFN, Via E. Fermi 40, Frascati, 00044, Italy marcelli@lnf.infn.it

^eRICMASS, Rome International Center for Materials Science Superstripes, Via dei Sabelli 119A, 00185 Rome, Italy.

Electronic Supplementary Information (ESI) available: [model structural parameters, photoreduction effects, and electronic structure including density of states and 3d electron localization function, charge transfer parameters]. See DOI: 10.1039/b000000x/

- 1 L.M. Milgrom, *The colours of life: an introduction to the chemistry of porphyrins and related compounds*, New York: Oxford University Press, 1997.
- 2 M.D. Lim, I.M. Lorkovic, K. Wedeking, A.W. Zanella, C.F. Works, S.M. Massick, P. C. Ford, *J. Am. Chem. Soc.*, 2002, 124, 9737-9743.
- 3 K. A. De Villiers and T. J. Egan, Recent advances in the discovery of haem-targeting drugs for malaria and schistosomiasis. *Molecules*, 2009, 14, 2868-2887.
- 4 A. Dorn, S. R. Vippagunta, H. Matile, C. Jaquet, J. L. Vennerstrom and R. G. Ridley, *Biochem. Pharmacol.*, 1998, 55, 727-736.
- 5 T. J. Egan, *J. Inorg. Biochem.*, 2008, 102, 1288-1299.
- 6 J. E. Penner-Hahn and K. O. Hodgson, *Iron Porphyrins*, Part III eds. A. B. P. Lever and A. B. Gray (New York: VCH Publishers) 235, 1989.
- 7 A. Bianconi, A. Congiu-Castellano, M. Dell'Ariceia, A. Giovannelli, P. J. Durham, E. Burattini and M. Barteri, *FEBS Lett.*, 1984, 178, 165-170.
- 8 P. D'Angelo, A. Lapi, V. Migliorati, A. Arcovito, M. Benfatto, O. M. Roscioni, W. Meyer-Klaucke and S. Della-Longa, *Inorg. Chem.*, 2008, 47, 9905-9918.
- 9 B. M. Leu, J. T. Sage, N. J. Silvernail, W. R. Scheidt, A. Alatas, E. E. Alp and W. Sturhahn, *J. Phys. Chem. B*, 2011, 115, 4469-4473.
- 10 D. Kim, D. Holten and M. Gouterman, *J. Am. Chem. Soc.*, 1984, 106, 2793-2798.
- 11 C. Consani, G. Auböck, F. van Mourik and M. Chergui, *Science*, 2013, 339, 1586-1589.
- 12 Z.-L. Cai, M. J. Crossley, J. R. Reimers, R. Kobayashi and R. D. Amos, *J. Phys. Chem. B*, 2006, 110, 15624-15632.
- 13 I. Duchemin, T. Deutsch and X. Blase, *Phys. Rev. Lett.*, 2012, 109, 167801-167806.
- 14 C. Hu, B. C. Noll, P. M. B. Piccoli, A. J. Schultz, C. E. Schulz and W. R. Scheidt, *J. Am. Chem. Soc.*, 2008, 130, 3127-3136.
- 15 S.A. Wilson, E. Green, I.I. Mathews, M. Benfatto, K.O. Hodgson, B. Hedman and R. Sarangi, *Proc. Natl. Acad. Sci. U S A*, 2013, 110, 16333-16338.
- 16 K. Dziedzic-Kocurek, D. Okla and J. Stanek, *Nukleonika*, 2013, 58, 7-11.
- 17 K. Dziedzic-Kocurek, H. J. Byrne, A. Swiderski and J. Stanek, *Acta Phys. Pol. A*, 2009, 115, 552-555.
- 18 S. A. Suchkova, A. Soldatov, K. Dziedzic-Kocurek and M. J. Stillman, *J. Phys: Conf. Ser.*, 2009, 190, 012211-012214.

- 19 J. Stanek and K. Dziedzic-Kocurek, *J. Magn. Magn. Mater.*, 2010, 322, 999-1003.
- 20 K. Dziedzic-Kocurek, D. Okla and J. Stanek, *Nukleonika*, 2013, 58, 83-86.
- 21 John J. Rehr, Joshua J. Kas, Fernando D. Vila, Micah P. Prange and K. Jorissen, *Phys. Chem. Chem. Phys.*, 2010, 12 5503-5513.
- 22 L. Hedin and S. Lundqvist, in *Solid State Physics*, eds. D. T. Frederick Seiz and E. Henry, Academic Press, 1970, 1-181.
- 23 A.L. Ankudinov, B. Ravel, J.J. Rehr and S.D. Conradson, *Phys. Rev. B*, 1998, 58, 7565-7576.
- 24 J. Clark Stewart, D. Segall Matthew, J. Pickard Chris, J. Hasnip Phil, I. J. Probert Matt, K. Refson and C. Payne Mike, *Z. Kristallogr.*, 2005, 220, 567-570.
- 25 D. M.Ceperley, B. J. Alder, *Phys. Rev. Lett.*, 1980, 45, 566-569.
- 26 J. P. Perdew, A. Zunger, *Phys. Rev. B*, 1981, 23, 5048-5079.
- 27 D. Vanderbilt, *Phys. Rev. B*, 1990, 41, 7892-7895.
- 28 J. Barbee and A. E. Kuznetsov, *Computational & Theoretical Chemistry*, 2012, 981, 73-85.
- 29 P. Rydberg and L. Olsen, *The Journal of Physical Chemistry A*, 2009, 113, 11949-11953.
- 30 M. Nakamura, *Coord. Chem. Rev.*, 2006, 250, 2271-2294.
- 31 D.F. Koenig, *Acta Cryst.*, 1965, 18, 663-673.
- 32 L. Cheng, J. Lee, D.R. Powell, and G.B. Richter-Addo, *Acta Cryst. E*, 2004, 60, m1340-m1342.
- 33 W.R. Scheidt and M.G. Finnegan, *Acta Cryst. C*, 1989, 45, 1214-1216.
- 34 P.N. Swepston and J. Albers, *Acta Cryst. C*, 1985, 41, 671-673.
- 35 Z.Y. Wu, D.C. Xian, T.D. Hu, Y.N. Xie, Y. Tao, C.R. Natoli, E. Paris and A. Marcelli, *Phys. Rev. B*, 2004, 70, 033104-033107.
- 36 I. Viciano, S. Berski, S. Marti and J. Andres, *J. Comput. Chem.*, 2013, 34,780-789.